

SCIENTIFIC REPORTS



OPEN

Fabrication, Optimization and Characterization of Natural Dye Sensitized Solar Cell

William Ghann, Hyeonggon Kang, Tajbik Sheikh, Sunil Yadav, Tulio Chavez-Gil, Fred Nesbitt & Jamal Uddin

Received: 27 June 2016
Accepted: 20 December 2016
Published: 27 January 2017

The dyes extracted from pomegranate and berry fruits were successfully used in the fabrication of natural dye sensitized solar cells (NDSSC). The morphology, porosity, surface roughness, thickness, absorption and emission characteristics of the pomegranate dye sensitized photo-anode were studied using various analytical techniques including FESEM, EDS, TEM, AFM, FTIR, Raman, Fluorescence and Absorption Spectroscopy. Pomegranate dye extract has been shown to contain anthocyanin which is an excellent light harvesting pigment needed for the generation of charge carriers for the production of electricity. The solar cell's photovoltaic performance in terms of efficiency, voltage, and current was tested with a standard illumination of air-mass 1.5 global (AM 1.5G) having an irradiance of 100 mW/cm². After optimization of the photo-anode and counter electrode, a photoelectric conversion efficiency (η) of 2%, an open-circuit voltage (V_{oc}) of 0.39 mV, and a short-circuit current density (I_{sc}) of 12.2 mA/cm² were obtained. Impedance determination showed a relatively low charge-transfer resistance (17.44 Ω) and a long lifetime, signifying a reduction in recombination losses. The relatively enhanced efficiency is attributable in part to the use of a highly concentrated pomegranate dye, graphite counter electrode and TiCl₄ treatment of the photo-anode.

Solar energy is rapidly becoming the most viable, eco-friendly and sustainable alternate source of renewable energy¹. There has been an exponential growth in the production of solar cells over the past two decades^{1–3}. One of the most promising means of solar energy conversion is the use of dye-sensitized solar cells (DSSC) first developed by Grätzel *et al.* in 1991 and has attracted much attention in the last couple of decades leading to a plethora of publications on the subject^{4–10}. The interest in DSSC and more precisely Natural Dye Sensitized Solar Cell (NDSSC) is mainly due to its low cost of fabrication and environmental friendly nature^{11,12}.

Currently, DSSC has the potential to convert photons from sunlight to electrical energy at 13% efficiency¹³. An intensive effort has been directed towards the optimization of the various components of DSSC with the goal of fabricating more efficient and stable cells. The DSSC as displayed in Fig. 1 is composed of a redox couple electrolyte system, typically iodide and triiodide complex, sandwiched between two glass plates, a photo-anode and a counter electrode. The redox couple in the electrolyte is used to regenerate the oxidized dye. The photo-anode consist of glass plate coated with a thin layer of transparent conductive oxide (Fluorine doped tin-oxide, FTO or Indium doped tin-oxide, ITO) and a monocrystalline semiconductor (usually titanium dioxide, TiO₂) which serves as a scaffold for the dye sensitizer. The counter electrode is also made up FTO covered glass slide coated usually with a thin film of Platinum or Carbon for the catalysis of the redox reaction with electrolyte.

The total efficiency of the DSSC is dependent on the nature, optimization and compatibility of each one of the components of the solar cell and more particularly the photo-anode which plays a vital role in the charge generation and transfer processes. To increase the power conversion efficiency of DSSC, a nanostructured porous titanium dioxide with a wide band gap and large exciton binding energy is typically used in constructing the photo-anode. The large surface area of the nanostructured TiO₂ insures the adsorption of sufficiently large number number of dye molecules for efficient harvesting of radiant energy. The dye, typically, with a wide and intense absorption spectrum is adsorbed on the TiO₂ via anchoring groups such as carboxylic, carbonyl and hydroxyl located on the dye molecule. A strong adsorption of the dye unto the nanostructured TiO₂ is required for the efficient electron injection into the conduction band of the TiO₂ semiconductor.

Center for Nanotechnology, Department of Natural Sciences, Coppin State University, 2500 W. North Ave, Baltimore, MD, USA. Correspondence and requests for materials should be addressed to J.U. (email: juddin@coppin.edu)

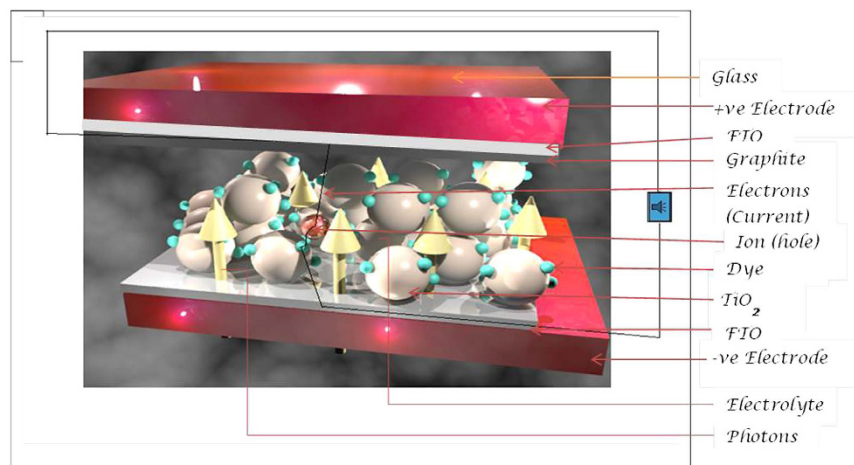


Figure 1. 3D-diagram illustrating a magnified cross-section of Dye Sensitized Solar Cell (DSSC).

The dye sensitizer anchored on the surface of titanium dioxide absorbs photons and gets electronically excited. Energy is produced when the excited electron moves from the valence band to the conduction band of the semiconductor. The electrolyte (I^-/I_3^-) donates electron back to the dye. The sensitizers currently used in the fabrication of solar cells are transition metal coordination complexes such as Ruthenium (II) carboxylated polypyridyl complexes, due to their intense charge-transfer absorption in the whole visible range and highly efficient metal-ligand charge transfer transition (MLCT)^{14,15}. Natural dyes are however more desirable than these synthetic dyes because they are more economical, easily attainable, and abundant in supply and environmentally friendly^{5,16}. In addition, they turn to have large absorption coefficient owing to allowed π to π^* transitions.

The performance of various natural dye containing pigments such as anthocyanin^{17,18}, xanthene¹⁴, chlorophyll, carotenoid and flavonoid have been thoroughly investigated¹¹. These pigments are derived from various plant parts such as flower petals, leaves, roots and fruits pulp/bark.

In this study, juice extracted from pomegranate was investigated as potent sensitizer for DSSC in comparison to other natural dyes. The pomegranate is a rich source of anthocyanin and we have deployed it as a sensitizer for the absorption of photons in DSSCs in the generation of electricity¹⁹. Anthocyanins are polyphenolic ring-based flavonoids widely known for their antioxidant properties²⁰. They differ from other flavonoids by the presence of a positive charge in the central ring structure and are responsible for the intense colors of other fruits and vegetables such as the berries and red cabbages²⁰. They have been shown to display a wide absorption/emission band in the UV-Visible region of the spectrum as a result of electron charge transfer transitions^{16,21}.

Results and Discussion

Absorption spectra. The overall performance of a DSSC is reliant on the light absorption capability of the dye sensitizer and the diffusion of the ejected electron through the mesoporous TiO_2 film. The optical properties of the dye extracted from pomegranate were investigated using UV-vis spectrometry. The absorption spectra of pomegranate dye extract, bare TiO_2 and pomegranate dye/ TiO_2 films are illustrated in Fig. 2a. The Pomegranate dye extract exhibited an intense absorption broad band in the visible region with a peak at 510 nm. This intense absorption in the visible region (510 nm) matches with that reported for anthocyanin and is the reason for the efficient harvesting of photons in NDSSC¹⁹. Plant parts containing anthocyanins have been widely investigated for use as photosensitizers in the fabrication of NDSSC. In addition to their high absorption coefficient in the visible region of the electromagnetic spectrum, the presence of hydroxyl and carbonyl anchoring groups on anthocyanins enable their adsorption unto the surface of the TiO_2 . This adsorption facilitates the transfer of the injected electron from dye to the conduction band of TiO_2 which ultimately enhances the efficiency of NDSSC⁵. A non-zero absorbance was observed for the spectrum corresponding to pomegranate dye/ TiO_2 . The peak for anthocyanin in Pomegranate dye/ TiO_2 is not easily visible in the spectrum, nonetheless, a shift in the maximum wavelength is observed. The absorption band of the pomegranate dye has been reported to be red shifted to about 550 nm upon chelation to TiO_2 ²². The attachment of the anthocyanin containing dye onto TiO_2 has been suggested to have an effect on the HOMO and LUMO level of anthocyanin, which consequently decreases the band gap resulting in a redshift of the absorption peak²³. The peak in the ultra-violet region is prominent and shows a bathochromic shift from 275 nm to 285 nm. A non-zero absorption similar to that of pomegranate dye/ TiO_2 was also observed in spectrum of bare TiO_2 . The non-zero absorption has been attributed to diffused reflection of TiO_2 suspended in solvent. Due to the wideband gap of TiO_2 (3.2 eV), bare TiO_2 do not absorb visible light, hence, no absorption band is seen in the region extending from 400 nm to 700 nm as exhibited in Fig. 2a. Figure 2b shows the fluorescence spectra of pomegranate dye, pomegranate dye/ TiO_2 and bare TiO_2 employed in the fabrication of the NDSSC. The measurement was carried out with the exciting light in the range of $320 \text{ nm} \leq \lambda_{exc} \leq 600 \text{ nm}$.

Fourier Transformed Infrared (FTIR) Analysis. The IR spectra of the films annealed at room temperature shows three vibrational modes (Fig. 3a) which are ascribed to TiO_2 for ν_{O-H} at 3413 cm^{-1} , δ_{O-H} at 1622 cm^{-1} , and

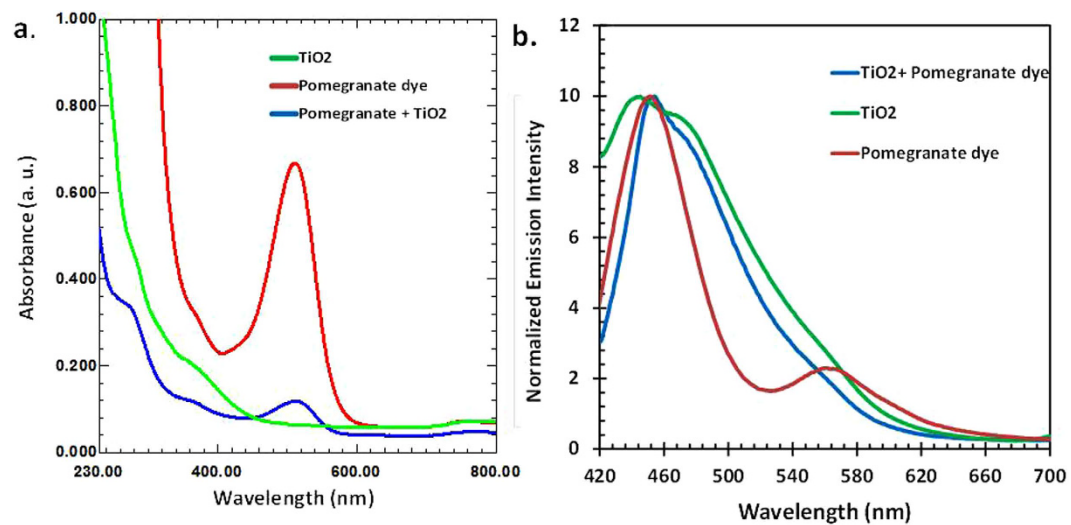


Figure 2. Absorption and emission spectra of bare titanium dioxide (green), pomegranate dye extract (red) and pomegranate sensitized TiO₂ film on FTO glass (blue). (a) Absorption spectra; (b) emission spectra.

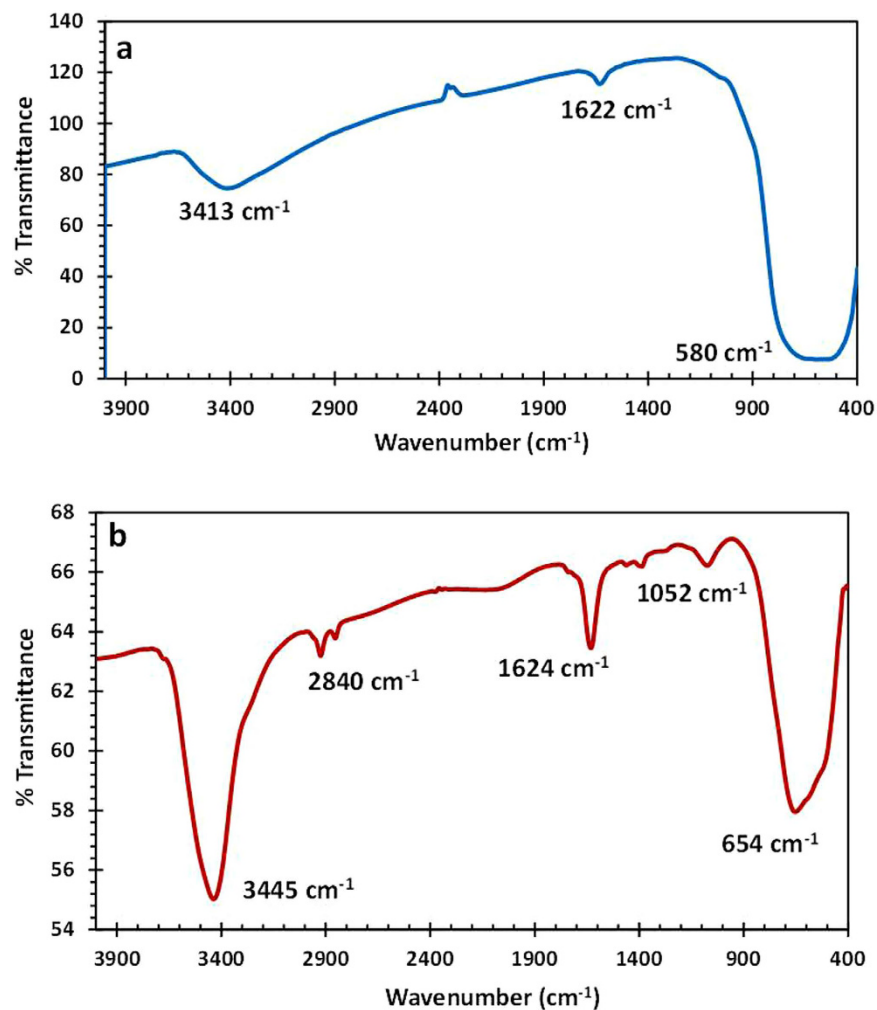


Figure 3. FT-IR spectrum of (a) TiO₂ and (b) TiO₂-POM film in KBr pellet.

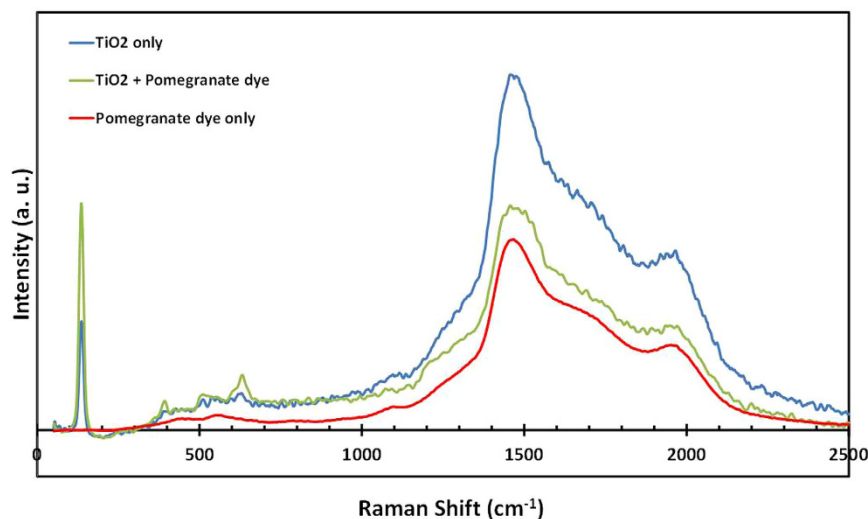


Figure 4. Raman spectra of sample films at room temperature of: TiO_2 (blue); and TiO_2 + Pomegranate dye (green); Pomegranate dye (red).

$\nu_{\text{Ti-O}}$ at 580 cm^{-1} as a broad stretching. The presence of pomegranate organic groups (Fig. 3b) such as hydroxyl, ethyl, acetyl and ethoxide in the films²³, shows stretchings for ν_{OH} at 3649 cm^{-1} , $\nu_{\text{O-H(water)}}$ at 3445 cm^{-1} , ν_{CH_2} , ν_{CH_3} at $2912, 2840\text{ cm}^{-1}$, δ_{CH_2} , δ_{CH_3} at $1463, 1367\text{ cm}^{-1}$, $\delta_{\text{C-C}}$ at 1710 cm^{-1} , $\delta_{\text{C=Cbenz}}$ at 1627 cm^{-1} , $\nu_{\text{C-O}}$ at 1052 cm^{-1} , and $\nu_{\text{Ti-O-C}}$ at 654 cm^{-1} , respectively. An interesting observation in these studies was that the stretching intensities were increased with the deposition of pomegranate dye, with a significant change on the TiO_2 IR modes, which indicates that there occurred an interaction that shift to low energies the initially TiO_2 stretching. This observation shows that the deposition of pomegranate dye undergoes strong phase transition due to an electronic environment change around the TiO_2 energies^{24–26}.

Raman Spectroscopy. To further evaluate the Pomegranate dye/ TiO_2 interaction in the nanocrystalline prepared films, Raman studies were performed in the range of $0\text{--}2500\text{ cm}^{-1}$ and the results are shown in Fig. 4. The D and G bands at 1470 cm^{-1} and 1960 cm^{-1} , respectively, have been previously attributed to the high disorder encountered for sp^3 carbons^{27,28}. The intense peak at 130 cm^{-1} assigned E_{g} is present in both of TiO_2 (blue) and the hybrid of TiO_2 and pomegranate (green), but it is absent in the measurement for pomegranate dye only. However, an interesting observation is that this 130 cm^{-1} peak, which is as a result of the symmetric stretching vibration of O-Ti-O in TiO_2 , is enhanced after the adsorption of the pomegranate dye. This observation proves that there is an interaction between the TiO_2 nanoparticles and the pomegranate dye. We speculate that the adsorbed pomegranate dye excited by the light source causes the enhancement of the E_{g} peak of TiO_2 .

Morphological Studies of the Fabricated Pomegranate Sensitized Solar Cell. Atomic force microscopy (AFM) images of the TiO_2 electrode, before and after the addition of pomegranate dye extract were obtained in order to examine the surface morphological characteristics of the nanocrystalline TiO_2 . The Fig. 5 shows the AFM images of bare TiO_2 and pomegranate dye sensitized TiO_2 on FTO glass (dye/ TiO_2). The images were obtained in $5\mu\text{m} \times 5\mu\text{m}$ and $2\mu\text{m} \times 2\mu\text{m}$ areas (Fig. 5a and b), analyzed to obtain insight the roughness and topographic features of the samples. Details of the surface structure of TiO_2 at the nanometer scale were observed. A high degree of roughness was observed on the surface of both bare TiO_2 and pomegranate dye/ TiO_2 . The Root mean square roughness of bare TiO_2 was about 197.6 nm in the $5\mu\text{m} \times 5\mu\text{m}$ scan area (Fig. 5a). Many TiO_2 clusters and cracks were found as exhibited in the topographic image and the image profile shown in Fig. 5(a–e). The rough surface of the TiO_2 increases the surface area of the film enabling more pomegranate dye to be adsorbed, which consequently increases the absorption of the incident light. The color distribution in the phase image of the dye/ TiO_2 was very uniform as shown in Fig. 5f, which is an indication that the pomegranate dye is uniformly distributed over the whole TiO_2 layer.

Field Emission Scanning Electron Microscopy Imaging. The morphological characteristics and elemental analysis of the TiO_2 photo-anode were investigated using Field-Emission Scanning Electron Microscopy (JSM 7100F, JEOL.COM) and Energy dispersive X-ray spectroscopy (EDS), respectively. No significant changes were observed in the surface morphology of the samples before and after dye sensitization. The Fig. 6a displays the FESEM image of the TiO_2 film with an adsorbed layer of pomegranate dye (pomegranate dye/ TiO_2). A highly porous network of nanocrystalline TiO_2 on FTO glass can be observed from the FESEM image. The EDS mapping analysis of the pomegranate dye/ TiO_2 (Fig. 6b) revealed the presence of carbon and Titanium, corresponding to the major elements present in pomegranate dye and TiO_2 , respectively. The carbon content of pomegranate dye/ TiO_2 in comparison with the bare TiO_2 was also investigated with EDS. The relatively intense carbon peak in the spectra of the dye-sensitized TiO_2 film (Fig. 6d) compared to the negligible carbon peak in spectra of the bare

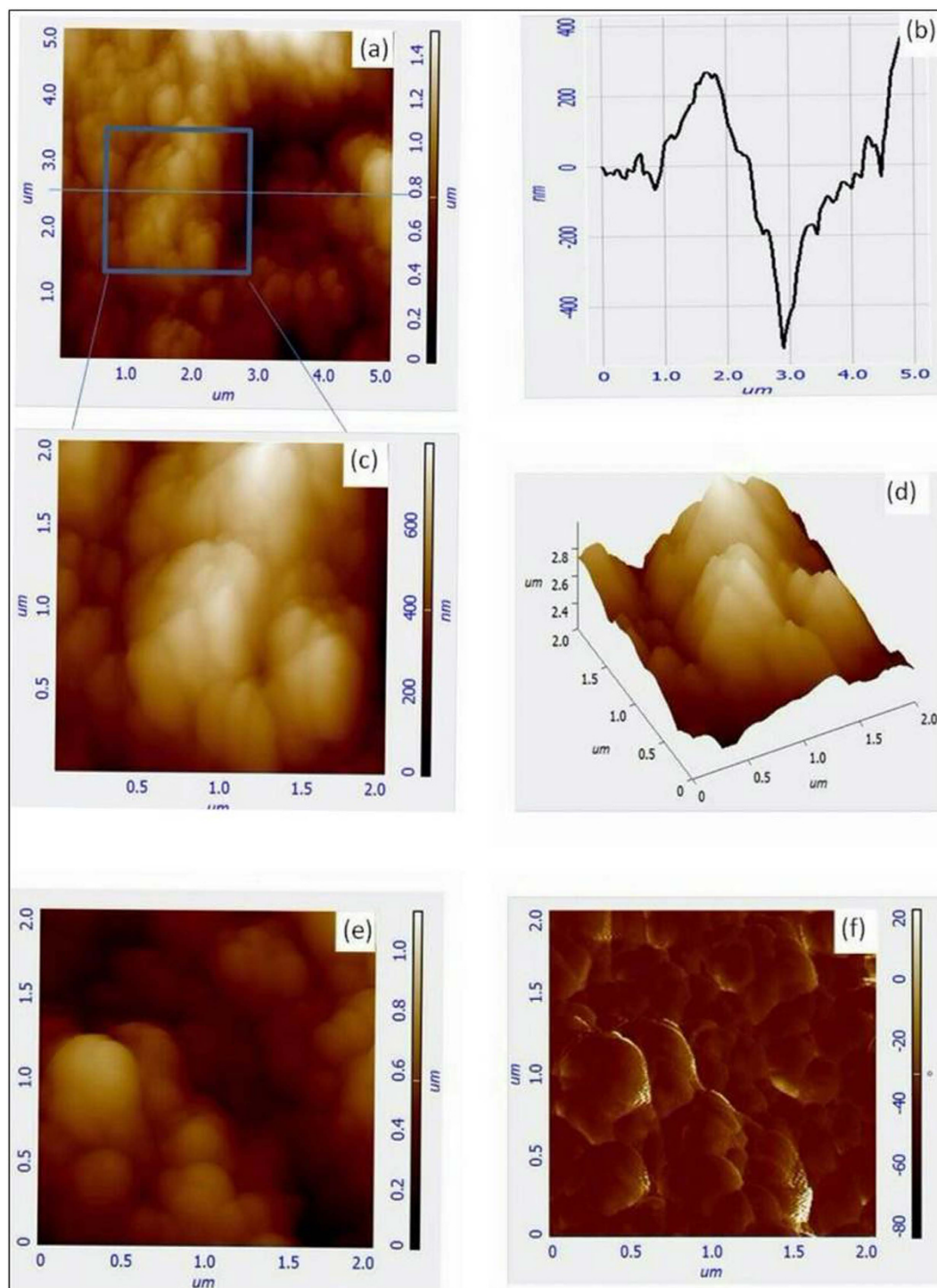


Figure 5. The AFM images of the bare TiO_2 and Dye/ TiO_2 samples. (a) Topographic image of TiO_2 (blue line for the cross-section analysis) in $5\ \mu\text{m} \times 5\ \mu\text{m}$; (b) Image profile of the TiO_2 topographic image; (c,d) 2D and 3D Topographic images of TiO_2 in $2\ \mu\text{m} \times 2\ \mu\text{m}$, respectively; (e,f) 2D Topographic and Phase images of Dye/ TiO_2 in $2\ \mu\text{m} \times 2\ \mu\text{m}$, respectively.

TiO_2 film (Fig. 6c) is indicative of a thorough adsorption of pomegranate dye onto the TiO_2 film. Although carbon and oxygen are the structural elements of the pigments present in the pomegranate dye, the peaks for oxygen are relatively the same in both EDS spectra (Fig. 6c and d) due to the oxygen component of TiO_2 .

The Fig. 6e shows a cross sectional view of the Dye/ TiO_2 sample exhibiting distinct layers of TiO_2 , FTO and the glass substrate. The elemental composition of the layers was confirmed by the EDS analysis and is displayed in Supplementary Fig. 7. The thickness of FTO on the glass was found to be about 500 nm (nominated size: 400 nm) and Dye/ TiO_2 film was found to be approximately $7\ \mu\text{m}$.

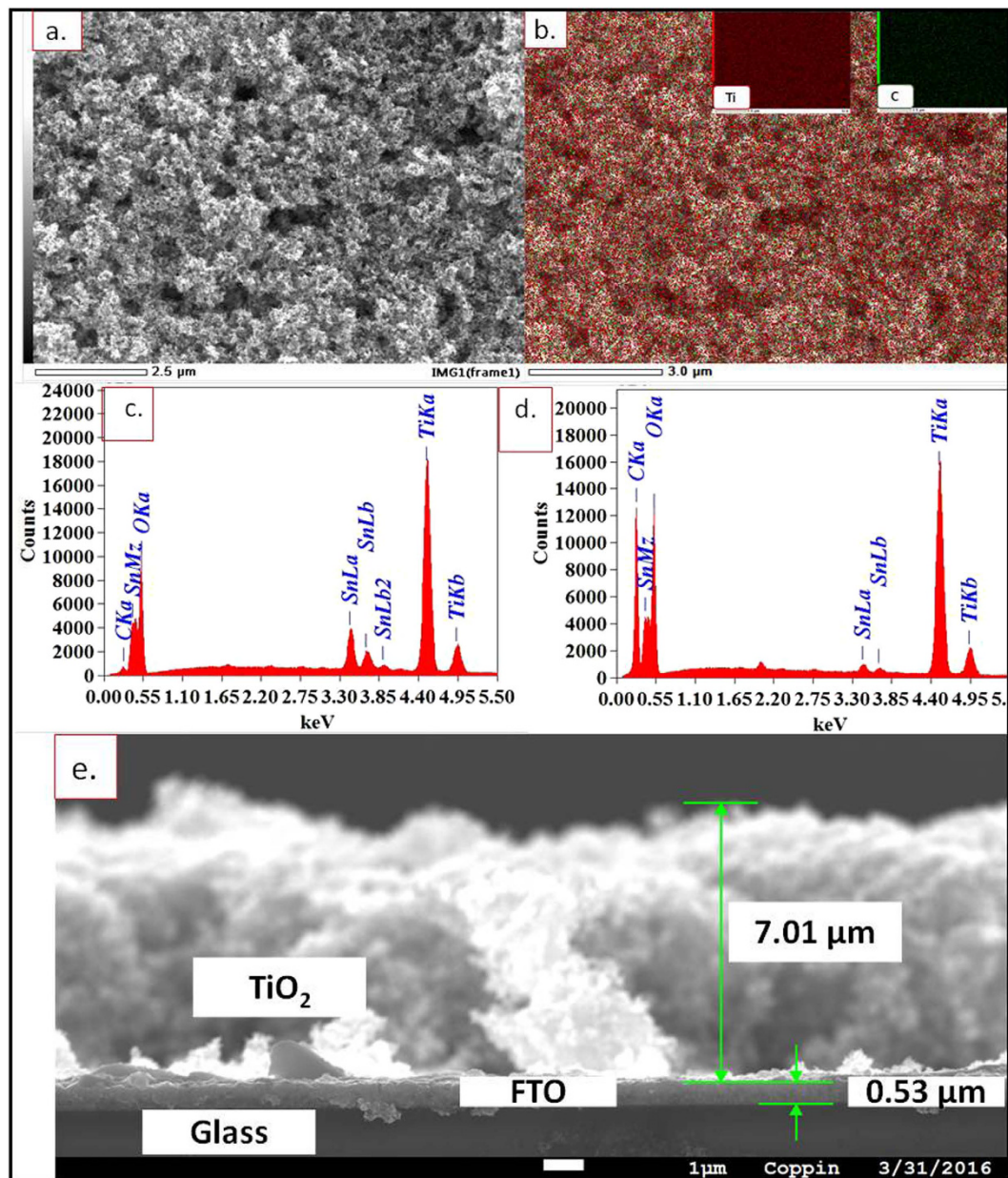


Figure 6. FESEM images of TiO₂ and Dye/TiO₂ samples. (a) Pomegranate dye sensitized FTO slide; (b) map analysis of pomegranate dye sensitized FTO slide; (c) EDS of bare TiO₂ coated FTO slide; (d) EDS of pomegranate sensitized FTO slide; (e) cross section of TiO₂ coated FTO slide.

As compared to the TiO₂ thin films prepared with other techniques such as the electrophoretic deposition method and the chemical reduction method, the TiO₂ film prepared by the spin coating method tend to possess a high void content, ample surface irregularities and a high degree of roughness, consistent with the findings of this imaging studies^{29,30}. Thus, the porous surface of the TiO₂ photo-anode suggests an enhancement in the adsorption of pomegranate dye into TiO₂ structure.

Transmission Electron Microscopy Imaging. The Transmission electron microscopy (TEM) images of the bare TiO₂ nanoparticles and the pomegranate dye sensitized TiO₂ nanoparticles are displayed in Fig. 7. A monodispersed layer of spherical TiO₂ nanoparticles with particle size in the range of 20–25 nm was observed (Fig. 7a and b). The Fig. 7c and d clearly show the presence small spherical nanoparticles, likely dye particles, with size in the range of 1–3 nm well distributed and decorated on the surface of the TiO₂ particles with a lattice fringe. These spherical nanoparticles were not observed on the bare TiO₂ nanoparticles as seen in the Fig. 7a and b which leads us to speculate that they are indeed dye particles. The interaction between the pomegranate dye and the TiO₂ nanoparticles results from the deprotonation of hydroxyl groups from the anthocyanin pigment.

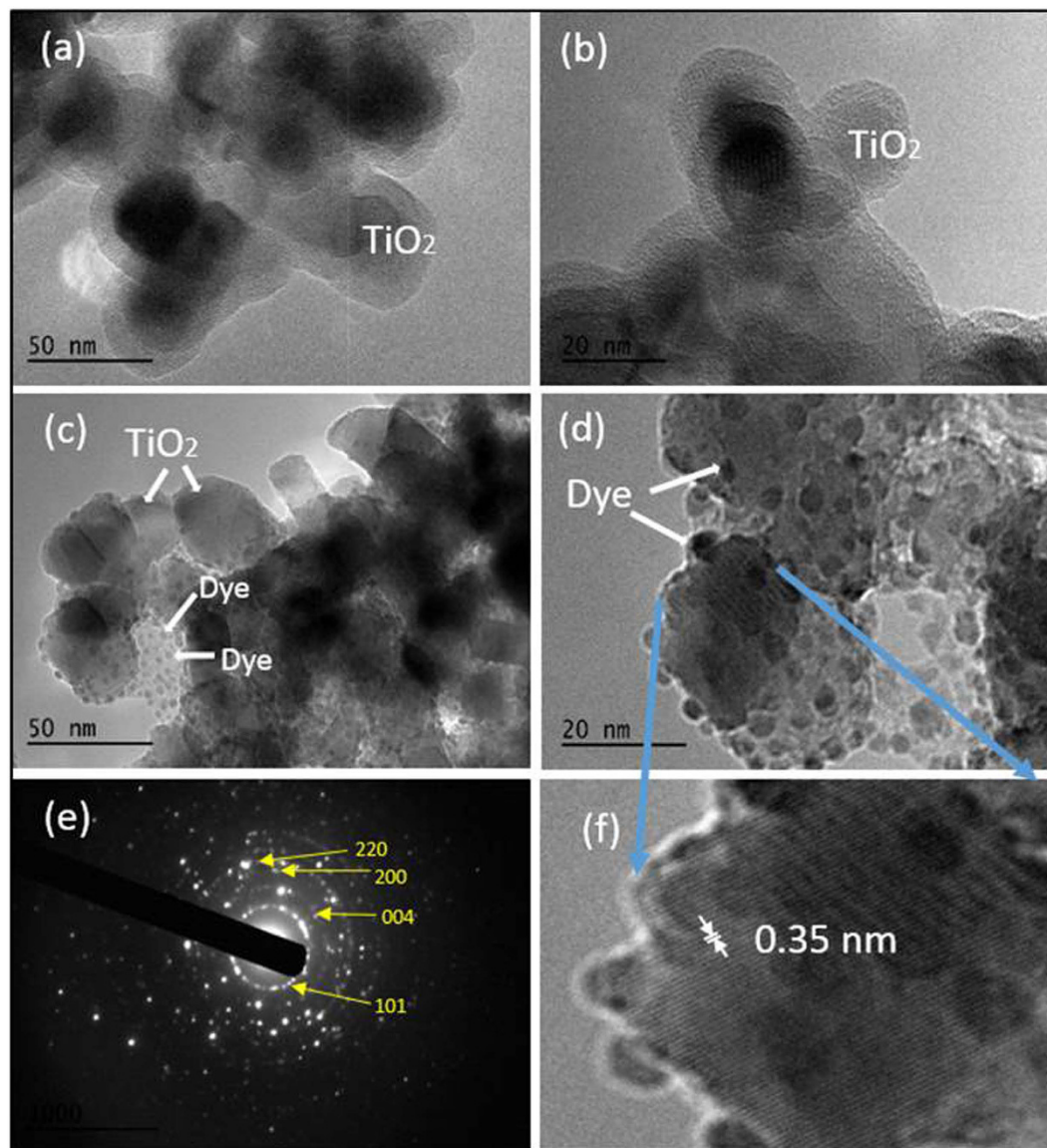


Figure 7. High-resolution TEM images of a TiO_2 and a pomegranate dye/ TiO_2 samples and a diffraction image of the TiO_2 : (a,b) high resolution TEM images of TiO_2 , (c,d) TEM of dye/ TiO_2 , (e) SAED pattern, (f) a zoom-in image showing the d-spacing value of the TiO_2 .

The selected area electron diffraction (SAED) pattern of the dye/ TiO_2 film as displayed in Fig. 7(e) shows the crystalline nature of the TiO_2 nanoparticles. The four bright concentric diffraction rings in the SAED can be indexed as the (101), (004), and (200) planes of the anatase TiO_2 , and (220) plane of the rutile TiO_2 . The HRTEM image of the TiO_2 /dye (Fig. 7d), displays the lattice fringe with an interlayer spacing of 0.3487 corresponding to the d-spacing of (101) planes in anatase TiO_2 as shown in the Fig. 7f.

Solar conversion efficiency measurement. The solar cell's photovoltaic performance in terms of efficiency, voltage, and current was tested with a standard illumination of air-mass 1.5 global (AM 1.5G) having an irradiance of 100 mW/cm^2 . After optimization of the photoanode and counter electrode, a photoelectric conversion efficiency (η) of 2%, an open-circuit voltage (V_{oc}) of 0.39 mV, and a short-circuit current density (I_{sc}) of 12.2 mA/cm^2 were obtained. The enhanced cell efficiency is attributed to the robust dye purification procedures adopted, treatment of anode with TiCl_4 and the use of graphite counter electrode. A further treatment of TiO_2 coated FTO glass with TiCl_4 has been shown to provide more sites for dye adsorption leading to high dye concentration that ensure the absorption of a greater amount of sunlight. The earlier fabrication carried out with just amorphous carbon and colloidal graphite (Fig. 8a) yielded 1.16% and 1.41% efficiencies, respectively. The improved efficiency obtained is also higher than a 1.5% efficiency of a pomegranate sensitized solar cell previously published by Bazargan *et al.*²². This efficiency is also higher than most natural dye sensitized solar cells as revealed in a review by Hug *et al.*¹¹ and other reviews in which percent efficiency of solar cell made from natural dyes were mostly less than one.

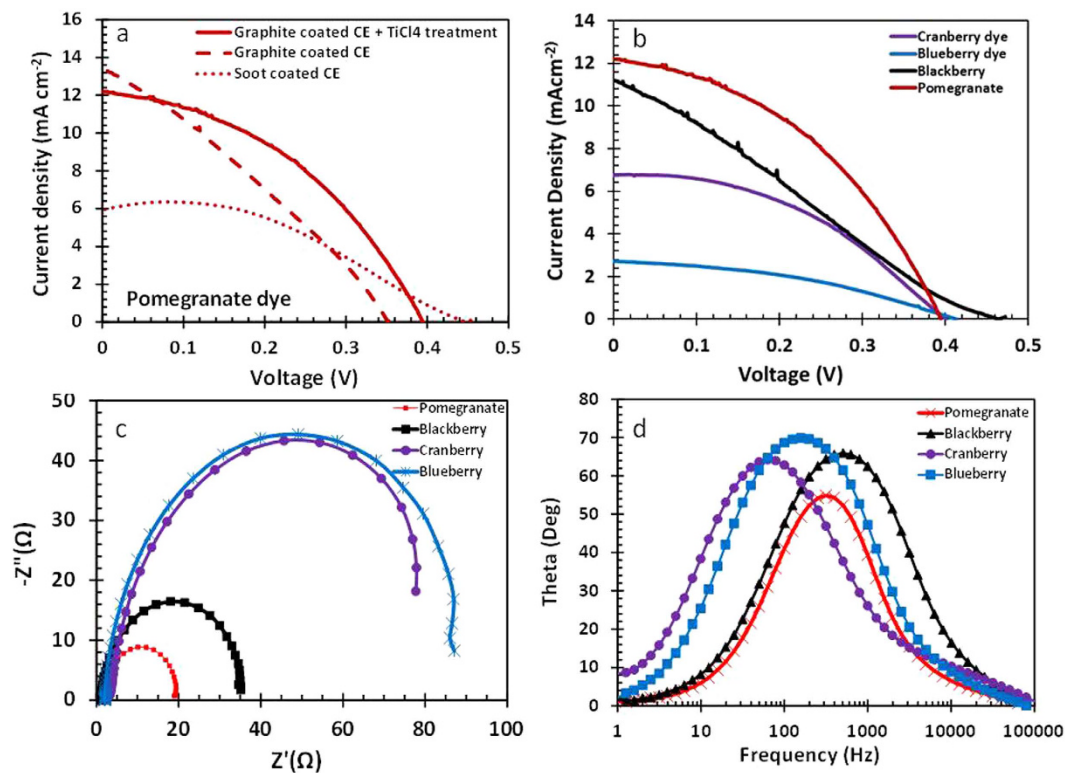


Figure 8. Photocurrent-voltage characteristics for dye sensitized solar cell measured under illumination of 100 W/cm^2 (1.5 AM): (a) Pomegranate dye sensitized solar cell with different electrodes; (b) Comparison of Pomegranate dye sensitized solar with other dyes; (c) Nyquist of different dye sensitized cells; (d) and Bode plots of Pomegranate, Blackberry, Cranberry and Blueberry dye sensitized cells.

	V_{oc} (V)	I_{sc} (mA/cm^2)	V_{mp} (V)	I_{mp} (mA/cm^2)	Fill Factor (%)	Efficiency (%)
Pomegranate	0.39	12.20	0.23	8.5	0.41	2.0
Blackberry	0.47	11.16	0.20	6.98	0.26	1.4
Cranberry	0.41	6.78	0.27	4.31	0.42	1.2
Blueberry	0.42	2.72	0.25	1.78	0.38	0.4

Table 1. Photovoltaic performance for fabricated pomegranate sensitized solar cell in comparison with other fabricated cell from the berry family (Blackberry, Raspberry, Blueberry and Cranberry).

The performance of the pomegranate dye as a potent sensitizer assessed in comparison with other dyes via the current, voltage, fill factor and conversion efficiency measurement are displayed in Table 1. The data shows that pomegranate sensitizer efficiency is far greater than that of berry fruit dyes employed in the study. The natural dyes studied included Blackberry, Cranberry and Blueberry dyes. Blackberry dye sensitized solar cell had the second highest efficiency (1.4%) followed by Cranberry sensitized solar cell (1.2%) and Blueberry dye sensitized solar cell (0.40%).

Electrochemical Impedance Analysis. The electrochemical impedance spectroscopy (EIS) has often been used to probe the kinetics and energetics of charge transport and recombination in dye sensitized solar cells. The EIS were recorded in the frequency range between 1 Hz and 100 KHz. Figure 8c shows the Nyquist plot of the various dye sensitized solar cells. Well-defined semicircles related to the charge transfer resistance between the counter electrode and redox (I^-/I_3^-) electrolyte are shown in the high frequency regions. In the EIS analysis, the pomegranate dye solar cell shows the smallest charge transfer resistance, $17.45 \text{ } \Omega$ compared to other dye cells: $85.38 \text{ } \Omega$ for blueberry, $68.94 \text{ } \Omega$ for cranberry, and $33.50 \text{ } \Omega$ for blackberry respectively. All natural dyes have anthocyanin a pigment responsible for the harvesting of radiant energy. Pomegranate having a large percentage of delphinidin possesses the ability to absorb more light than the other berries under consideration. This greater ability to absorb sunlight results in fast electron (hole) generation and transport, hence a lower hole-electron recombination in the cell. The light absorption is not as good in the berry fruit dye extract resulting in poor electron generation leading to relatively high resistance to the flow of electron at the $\text{TiO}_2/\text{dye}/\text{electrolyte}$ interphase.

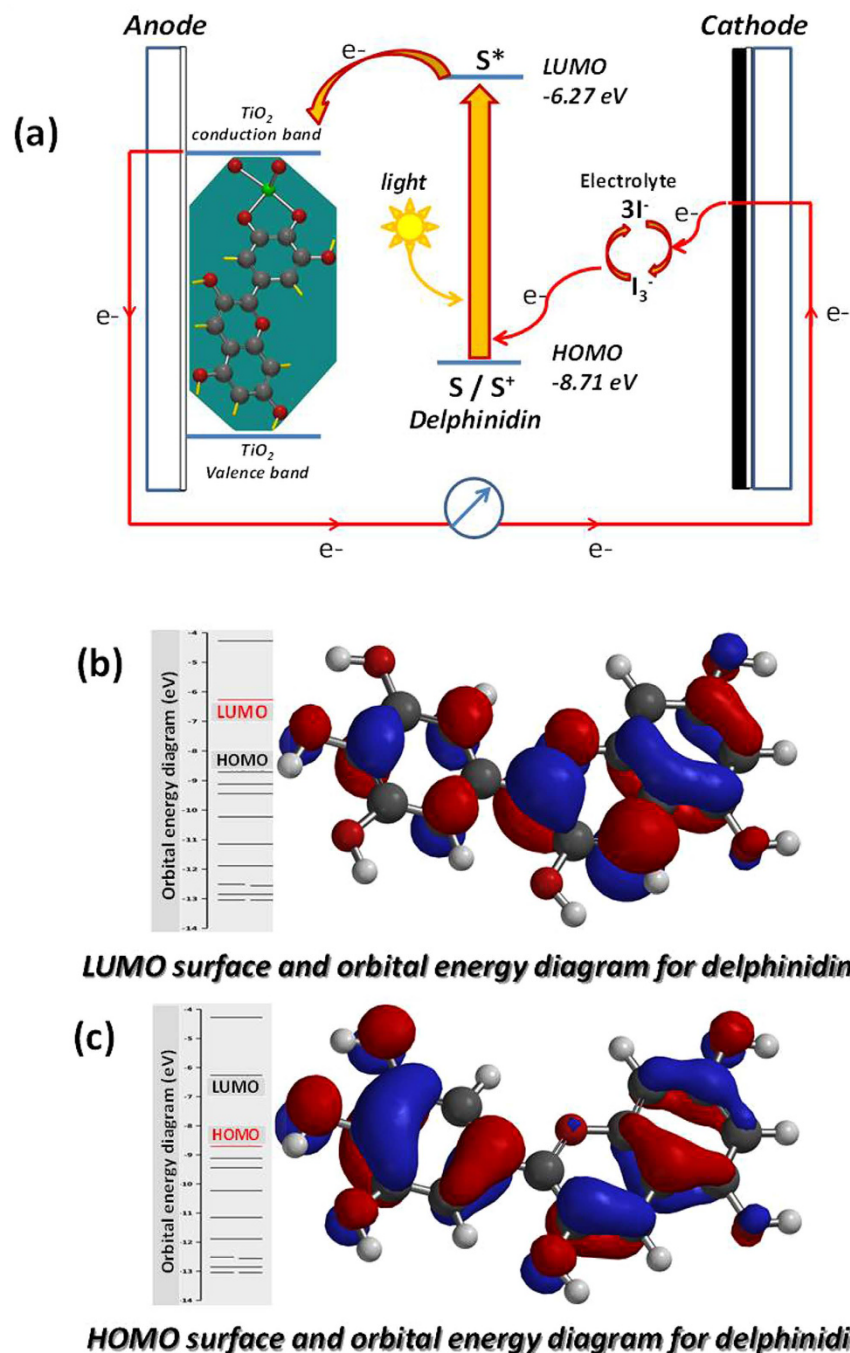


Figure 9. (a) Working principles of DSSC with delphinidin; (b) HOMO and (c) LUMO surface and orbital energy diagram for delphinidin.

Despite, the observed equivalence between the resistance for all the cell series, they do possess almost similar values. As shown in the I-V curve in the Fig. 8b, the pomegranate dye cell showed the highest efficiency because the low charge transfer resistance acted as the dominant factor affecting the performance of the natural dye sensitized solar cells. Figure 8d shows the Bode phase plot for the NDSSC. The blackberry dye showed a big phase shift in the high frequency region (the maximum frequency: 506 Hz) due to relatively small capacitance (52.8 μ F) compared to that of the other dyes. Overall the performance of the pomegranate DSSC is better than blackberry DSSC due to the electron transfer resistance of blackberry dye which is far higher than that of Pomegranate dye.

Working principle of Dye Sensitized Cell (DSSC). Upon illumination, dye molecules (S) adsorbed on the TiO₂ film absorb photon and are excited from the highest occupied molecular orbitals (HOMO) to the lowest unoccupied molecular orbital (LUMO) state as shown in Fig. 9(a). The photo-excited dye species (S*) injects an electron into the conduction band of TiO₂ electrode and becomes oxidized (S⁺). The oxidized dye species

subsequently accept an electron from the electrolyte (I^-) and the ground state of the dye (S) is restored. The injected electron percolates through the mesoporous TiO_2 film to the FTO layer and is transported through an external circuit to a load where the work done is delivered as electrical energy. The electron from the external load diffuses to the cathode where it gets transferred to the electrolyte, (I_3^-) so the electrolyte system is regenerated. Density Functional Theory (DFT) calculations were used to optimize the geometry of delphinidin molecule using the software Spartan' 14 from Wavefunction, Inc. Irvine, CA, USA. These calculations were used to determine the highest occupied molecular orbital (HOMO) and the lowest unoccupied molecular orbital (LUMO) energies of delphinidin dye. The anthocyanidin, delphinidin, was chosen for the calculations because it has been shown that its derivative, delphinidin -3, 5-diglucoside is the predominant anthocyanin present in pomegranate dye extract. The calculations gave a result for the HOMO of -8.71 eV and the result for the LUMO of -6.27 eV. The difference in the HOMO and LUMO, which is the energy band gap, was found to be 2.44 eV.

The HOMO and LUMO surfaces and orbital energy diagrams are shown in Fig. 9(b and c) respectively. In Fig. 9(b and c), the blue and red regions represent positive and negative values of the orbitals, respectively.

Conclusion

Dye extract from pomegranate fruit was utilized as the light-harvesting analog in the fabrication of a low cost, eco-friendly dye-sensitized solar cell. The chemical, structural, morphology and optical properties of the pomegranate/ TiO_2 coated FTO glass were investigated via atomic force microscopy, field emission scanning electron microscopy, energy-dispersive x-ray spectroscopy, uv-vis and fluorescence spectroscopy. The fabricated DSSC showed an enhanced solar-to-electrical energy conversion. Theoretical calculation on delphinidin, an anthocyanin derivative found in pomegranate resulted in a HOMO of -8.71 eV and LUMO of -6.27 which makes it possible for effective electron transfer of charge from the LUMO of the pomegranate into the conduction band of TiO_2 . The regeneration of the dye by the redox electrolyte (I^-/I_3^-) coupling increases the lifetime of the dye. Also the narrower band gap of delphinidin (2.44 eV) increases the intramolecular electronic transition probabilities. The efficiency of the prepared pomegranate sensitized solar cell was $\eta = 2.0\%$, and fill factor $FF = 0.41$ with the short circuit current (I_{sc}) and open circuit voltage (V_{oc}) being 12.2 mA/cm² and 0.39 V respectively. The excellent photovoltaics performance of the solar cell could be attributed to the high concentration of anthocyanins present in pomegranate dye used in the sensitization of the nanocrystalline TiO_2 . The use of graphite as the counter electrode and $TiCl_4$ treatment of the photo-anode improved the solar cell efficiency by more than one percent.

Experimental Methods

Materials. Titanium dioxide powder (Degussa P-25) was purchased from the institute of chemical education, university of Wisconsin-Madison, department of chemistry, Madison, WI, USA. Fluorine tin oxide (FTO) conducting glass slides were purchased from Harford glass company, Hartford City, Indiana, USA. Sodium Hydroxide (NaOH), acetone (C_3H_6O), ethanol (C_2H_5OH) and acetic acid (CH_3CO_2H) were purchased from Sigma-Aldrich (St. Louis, MS, USA) and were used without further purification.

Characterization techniques. The morphology of each film was analyzed using field emission scanning electron microscopy (Model FESEM: JSM-7100FA JEOL USA, Inc.). The surface morphological characteristics of the nanocrystalline TiO_2 were experimentally evaluated using Atomic Force Microscopy (AFM) manufactured by NT-MDT (Model: Solver next, NT-MDT). Absorption spectroscopy was carried out with UV-3600 Plus from Shimadzu, MD, USA. Emission spectroscopy was measured with RF-5301PC from Shimadzu, MD, USA. (Raman Studies was carried A model DXR smart Raman spectrometer (Thermo Fisher Scientific Co., Ltd., USA). ATR spectra were obtained with a Thermo Nicolet iS50 FTIR.) Transmission Electron Microscopy (TEM) images were acquired on JEM-1400 PLUS (JEOL USA, Peabody, Massachusetts, USA). The images were viewed using Digital Micrograph software from GATAN (GATAN Inc., Pleasanton, CA, USA). TiO_2 paste was printed on FTO glass using WS-650 Series Spin Processor from Laurell Technologies Corporation, PA, USA. Carbon paint used in making cathode slides was purchased from TED PELLA, INC, USA. The cell performance was measured using 150 W fully reflective solar simulator with a standard illumination of air-mass 1.5 global (AM 1.5 G) having an irradiance of 100 mW/cm² (Sciencetech Inc.), London, Ontario, Canada. Reference 600 Potentiostat/Galvanostat/ZRA from GAMRY Instruments (Warminster, PA). HOMO and LUMO calculations were carried out using Spartan'14 software from Wavefunction, Inc. Irvine, CA, USA.

Natural Dye Extraction. A fresh pomegranate and berry fruits were peeled and the juice extracted from the pulp coats using a commercial fruit juice extractor. The extraction was followed by a sequence of filtration, centrifugation, and decantation to remove any precipitate present in the crude extract.

Fabrication of NDSSC. The electrodes were prepared according to a previously published procedure with some modification³¹. The Supplementary Fig. S1 shows a schematic of the stages involved in the fabrication of the pomegranate dye sensitized solar cell. The working electrode was prepared by depositing a thin film of TiO_2 on the conductive side of a fluorine doped tin oxide (FTO) glass using a spin coater and annealing the film at 380 °C for 2 hours. The TiO_2 coated FTO glass was subsequently dipped in $TiCl_4$ solution for an hour and annealed again for 30 minutes. The substrate was then immersed in a freshly squeezed pomegranate juice for dye sensitization. To concentrate the sample, pomegranate juice was lyophilized and dissolved in a minimum amount of water before dye sensitization. The counter electrode (cathode) was prepared by either depositing carbon soot on FTO glass slide or painting this glass slide with colloidal graphite. The pomegranate dye sensitized and the carbon electrodes were assembled to form a solar cell by sandwiching a redox (I^-/I_3^-) electrolyte solution as displayed in Supplementary Fig. S1.

References

- Singh, G. K. Solar power generation by PV (photovoltaic) technology: A review. *Energy* **53**, 1–13 (2013).
- Chen, W. *et al.* Efficient and stable large-area perovskite solar cells with inorganic charge extraction layers. *Science* **350**, 944–948 (2015).
- Yoo, K. *et al.* Completely Transparent Conducting Oxide-Free and Flexible Dye-Sensitized Solar Cells Fabricated on Plastic Substrates. *ACS Nano* **9**, 3760–3771 (2015).
- O'Regan, B. & Gratzel, M. A low-cost, high-efficiency solar cell based on dye-sensitized colloidal TiO₂ films. *Nature* **353**, 737–740 (1991).
- Narayan, M. R. Review: Dye sensitized solar cells based on natural photosensitizers. *Renew Sust Energy Rev* **16**, 208–215 (2012).
- Hao, S., Wu, J., Huang, Y. & Lin, J. Natural dyes as photosensitizers for dye-sensitized solar cell. *Sol. Energy* **80**, 209–214 (2006).
- Shalini, S., Balasundara prabhu, R., Prasanna, S., Mallick, T. K. & Senthilarasu, S. Review on natural dye sensitized solar cells: Operation, materials and methods. *Renew Sust Energy Rev* **51**, 1306–1325 (2015).
- Sugathan, V., John, E. & Sudhakar, K. Recent improvements in dye sensitized solar cells: A review. *Renew Sust Energy Rev* **52**, 54–64 (2015).
- Bahadur, K. I., Jyoti, N. J., Kumar, M. P. & Suman, C. Dye-Sensitized Solar cell using extract of Punica Granatum L. Pomegranate (Bedana) as a Natural Sensitizer. *Research of J. Chem. Sci.* **2**, 81–83 (2012).
- Meyer, G. J. The 2010 Millennium Technology Grand Prize: Dye-Sensitized Solar Cells. *ACS Nano*. **4**, 4337–4343 (2010).
- Hug, H., Bader, M., Mair, P. & Glatzel, T. Biophotovoltaics: Natural pigments in dye-sensitized solar cells. *Appl. Energy* **115**, 216–225 (2014).
- Ludin, N. A. *et al.* Review on the development of natural dye photosensitizer for dye-sensitized solar cells. *Renew Sust Energy Rev*. **31**, 386–396 (2014).
- Mathew, S. *et al.* Dye-sensitized solar cells with 13% efficiency achieved through the molecular engineering of porphyrin sensitizers. *Nat. Chem.* **6**, 242–247 (2014).
- Karki, I. B., Nakarmi, J. J., Mandal, P. K. & Chatterjee, S. Absorption Spectra of Natural Dyes and Their Effect on Efficiency of ZnO Based Dye-Sensitized Solar Cells. *NJST* **13**, 179–185 (2013).
- Duffy, N. W., Peter, L. M., Rajapakse, R. M. G. & Wijayantha, K. G. U. Investigation of the Kinetics of the Back Reaction of Electrons with Tri-Iodide in Dye-Sensitized Nanocrystalline Photovoltaic Cells. *The J. Phys. Chem B*. **104**, 8916–8919 (2000).
- Hosseinnezhad, M., Moradian, S. & Gharanjig, K. Fruit extract dyes as photosensitizers in solar cells. *Curr. Sci.* **109**, 953–956 (2015).
- Dai, Q. & Rabani, J. Photosensitization of nanocrystalline TiO₂ films by anthocyanin dyes. *J. of Photochem. Photobiol.* **148**, 17–24 (2002).
- Dai, Q. & Rabani, J. Photosensitization of nanocrystalline TiO₂ films by pomegranate pigments with unusually high efficiency in aqueous medium. *Chem Commun.* **20**, 2142–2143 (2001).
- Noda, Y., Kaneyuki, T., Mori, A. & Packer, L. Antioxidant activities of pomegranate fruit extract and its anthocyanidins: delphinidin, cyanidin, and pelargonidin. *J Agric Food Chem.* **50**, 166–171 (2002).
- Hou, D.-X., Fujii, M., Terahara, N. & Yoshimoto, M. Molecular Mechanisms Behind the Chemopreventive Effects of Anthocyanidins. *J Biomed Biotechnol.* **2004**, 321–325 (2004).
- Cherepy, N. J., Smestad, G. P., Grätzel, M. & Zhang, J. Z. Ultrafast Electron Injection: Implications for a Photoelectrochemical Cell Utilizing an Anthocyanin Dye-Sensitized TiO₂ Nanocrystalline Electrode. *J. Phys. Chem B*. **101**, 9342–9351 (1997).
- Bazargan, M. H., Byranvand, M., Kharat, N. & Fathollahi, L. *Optoelectron Adv Mat.* **5**, 360–362 (2011).
- Li, N., Pan, N., Danhong, Li & Lin, S. Natural Dye-Sensitized Solar Cells Based on Highly Ordered TiO₂ Nanotube Arrays. *Int. J. Photoenergy.* **598753**, 1–5 (2013).
- Sivaranjani, K. & Gopinath, C. S. Porosity driven photocatalytic activity of wormhole mesoporous TiO₂-xNx in direct sunlight. *J. Mater. Chem.* **21**, 2639–2647, (2011).
- Kumar, P. M., Badrinarayanan, S. & Sastry, M. Nanocrystalline TiO₂ studied by optical, FTIR and X-ray photoelectron spectroscopy: correlation to presence of surface states. *Thin Solid Films* **358**, 122–130 (2000).
- Zhang, J.-Y. *et al.* Nanocrystalline TiO₂ films studied by optical, XRD and FTIR spectroscopy. *J. Non-Cryst. S* **303**, 134–138 (2002).
- Kudin, K. N. *et al.* Raman Spectra of Graphite Oxide and Functionalized Graphene Sheets. *Nano Let.* **8**, 36–41 (2008).
- Maiaugree, W. *et al.* A dye sensitized solar cell using natural counter electrode and natural dye derived from mangosteen peel waste. *Sci Rep.* **5**, 15230, (2015).
- Voitchovsky, K. *et al.* In Situ Mapping of the Molecular Arrangement of Amphiphilic Dye Molecules at the TiO₂ Surface of Dye-Sensitized Solar Cells. *ACS Appl. Mater. Interfaces* **7**, 10834–10842 (2015).
- Lim, S. P., Pandikumar, A., Lim, H. N., Ramaraj, R. & Huang, N. M. Boosting Photovoltaic Performance of Dye-Sensitized Solar Cells Using Silver Nanoparticle-Decorated N, S-Co-Doped-TiO₂ Photoanode. *Sci Rep.* **5**, 11922 (2015).
- Amadi, L. *et al.* Creation of Natural Dye Sensitized Solar Cell by Using Nanostructured Titanium Oxide. *Nanosci. Nanoeng.* **3**, 25–35 (2015).

Acknowledgements

This work was financially supported by the University of Maryland System (Wilson E. Elkins Professorship), Constellation, an Exelon Company (E2- Energy to Educate grant program) and the United States Department of Education (USDE-SAFRA Title III Grant). The authors are also grateful to the Institution of Advancement, Coppin State University, for administrative help. The content is exclusively the responsibility of the authors and does not necessarily represent the official views of the funding agencies.

Author Contributions

J.U. conceived the idea and reviewed the final manuscript. W.G., T.S., H.K. designed the experiments. W.G., T.S. and S.Y. performed the experiments. W.G. and H.K. wrote the manuscript with the assistance of J.U. T.C.h.-G. performed Raman and FT-IR experiments and analysis., F.N. performed HOMO-LUMO theoretical calculation-analysis. All authors participated in the discussion and commented on the paper.

Additional Information

Supplementary information accompanies this paper at <http://www.nature.com/srep>

Competing financial interests: The authors declare no competing financial interests.

How to cite this article: Ghann, W. *et al.* Fabrication, Optimization and Characterization of Natural Dye Sensitized Solar Cell. *Sci. Rep.* **7**, 41470; doi: 10.1038/srep41470 (2017).

Publisher's note: Springer Nature remains neutral with regard to jurisdictional claims in published maps and institutional affiliations.



This work is licensed under a Creative Commons Attribution 4.0 International License. The images or other third party material in this article are included in the article's Creative Commons license, unless indicated otherwise in the credit line; if the material is not included under the Creative Commons license, users will need to obtain permission from the license holder to reproduce the material. To view a copy of this license, visit <http://creativecommons.org/licenses/by/4.0/>

© The Author(s) 2017